Fifty-first Annual Allerton Conference
Allerton House, UIUC, Illinois, USA
October 2 - 3, 2013

Virtual Oscillator Control for Voltage Source Inverters

Sairaj V. Dhople[†], Brian B. Johnson[♯], and Abdullah O. Hamadeh[‡]

Abstract— **This paper summarizes a suite of methods that have recently been proposed for the control and synchronization of parallel single- and three-phase voltage source power electronics inverters. Inspired by the phenomenon of synchronization in networks of coupled oscillators, the premise of the proposed *Virtual Oscillator Control* (VOC) is to control an inverter such that it mimics the dynamics of a nonlinear oscillator. Consequently, the inverters synchronize their voltage outputs and share the load power in proportion to their power ratings without any communication. The VOC design philosophy and sufficient conditions for global asymptotic synchronization are outlined. Simulations validate the analytical results for a parallel system of three-phase inverters serving a constant-power load.**

I. INTRODUCTION

This paper presents a suite of methods to synchronize and control a system of parallel single- and three-phase voltage-source inverters without communication. Drawing inspiration from the phenomenon of synchronization in networks of coupled oscillators, each inverter is controlled to emulate the dynamics of a nonlinear dead-zone oscillator. Leveraging the intrinsic electrical coupling between inverters, global asymptotic synchronization can be guaranteed with no additional communication. Additionally, the synchronization condition is demonstrated to be independent of the number of inverters in the system and the load characteristics. The proposed control paradigm is therefore robust (independent of load), resilient (requires no communication), and modular (independent of the number of inverters). The proposed method is referred as *virtual oscillator control* (VOC) to emphasize the fact that each inverter is digitally controlled to emulate the dynamics of a nonlinear oscillator.

Systems of parallel inverters are key constituents of distributed ac power systems in applications such as uninterruptible power supplies, microgrids, and renewable energy systems [1]–[8]. As will be demonstrated subsequently, VOC provides a number of system-level benefits in this setting including: i) minimizing communication between inverters, ii) maintaining system stability and synchronization in spite of load variations, iii) regulating the system voltage and frequency, and iv) ensuring the inverters share the load in proportion to their ratings.

Passivity-based methods were recently proposed in [9] to explore synchronization of coupled nonlinear oscillators with the goal of formulating control strategies for inverters in islanded power systems. The $\mathscr{L}_2$-based approach we adopt in this work to explore synchronization was outlined in [10], where sufficient conditions were derived for synchronization in a system of identical nonlinear oscillators connected to a common node through identical branch impedances. Subsequently in [11], we demonstrated applications of the oscillator-based controller in three-phase, low-inertia microgrids with high penetration of photovoltaic generation. In [10], [11], it was assumed that all inverters had identical power ratings and that the load was a passive impedance. Building on our previous efforts, in [12] we extended the synchronization condition to both linear and nonlinear loads, proposed a controller and output-filter design approach that promoted power sharing, and introduced a control method to facilitate the addition of inverters into an energized system with minimum transients. This paper provides an overview of the VOC-based inverter synchronization paradigm, and demonstrates applications of this method in a system of three-phase parallel inverters serving a constant power load.

Control strategies that do not necessitate communication in systems of parallel inverters have predominantly been inspired by the idea of droop control [13]–[20]. The fundamental premise of this method is to control the voltage and frequency of islanded inverters to be inversely proportional to the real and reactive power output, respectively [13], [21]–[23]. To overcome shortcomings associated with load-sharing accuracy and system frequency/voltage deviations, recent efforts have focused on the overlay of a communication network between inverters to implement secondary- and tertiary-level controls [15], [24]–[26]. In contrast, we have demonstrated experimentally that with VOC, the system frequency exhibits minimal deviations with variations in load, and the load voltage can be maintained between prescribed bounds without communication [12].

The remainder of this manuscript is organized as follows. Section II describes the nonlinear dead-zone oscillator that is employed in VOC, and provides a system-level description of the parallel system of single- and three-phase inverters that VOC is applied to. In Section III we outline sufficient synchronization condition for networks comprised of the nonlinear oscillators connected to a common node through identical branch impedances. Finally, the paper concludes with a simulation case study in Section IV.

[†]S. V. Dhople is with the Department of Electrical and Computer Engineering at the University of Minnesota, Minneapolis, MN. E-mail: sdhople@umn.edu

[♯]B. B. Johnson is with the Power Systems Engineering Center at the National Renewable Energy Laboratory, Golden, CO, but has written this article outside the scope of his employment. E-mail: brian.johnson@nrel.gov

[‡]A. O. Hamadeh is with the Department of Mechanical Engineering, Massachusetts Institute of Technology, Cambridge, MA. E-mail: ahamadeh@mit.edu

B. B. Johnson was supported in part by a National Science Foundation Graduate Research Fellowship and the Grainger Center for Electric Machinery and Electromechanics at the University of Illinois.

II. Oscillator Model Fundamentals

In this section, we first present the oscillator model that constitutes the mainstay of the proposed inverter control method. Next, we focus on how the inverters can be controlled to emulate the dynamics of the nonlinear dead-zone oscillators. Then, we provide an overview of the parallel system of single- and three-phase inverters that the VOC paradigm is applied to.

A. Oscillator Model

The nonlinear *dead-zone oscillator* that constitutes the basis of VOC is illustrated in Figure 1. Notice that the oscillator is composed of a resonant LC tank that sets the system frequency, a nonlinear voltage-dependent current source that sustains the oscillations, $g(\cdot)$, and a damping element, R. The terminology *dead-zone oscillator* follows from the fact that we can decompose g into a dead-zone function and a negative resistance. It is worth noting that many nonlinear electrical oscillators can be described in this format, i.e., a passive impedance connected in parallel to a nonlinear current source. However, the analytical approach we adopt in [10] imposes the requirement that the maximum slope of $g(\cdot)$ is bounded. Particularly, we require $\sigma = |\mathrm{d}g/\mathrm{d}v| < \infty$. (This requirement unfortunately disqualifies the application of some circuits, e.g., the well-known Van-der-Pol oscillator [27].) As described subsequently, the terminal voltage of the dead-zone oscillator is utilized to construct the PWM switching signals for the inverters. Consequently, it is important to ensure that the oscillator is tuned to operate in the quasi-harmonic region by minimizing the value of $\varepsilon := \sqrt{L/C}(\sigma - 1/R) > 0$ [28].

B. Description of Parallel Inverter System

The proposed VOC has been applied to systems of parallel inverters serving a common load. A representative schematic for a three-phase system is depicted in Fig. 2(a). To implement VOC, the nonlinear differential equations that govern the dynamics of the dead-zone oscillator in Fig. 1 are programmed into the digital controllers of the inverters. Figures 4(a) and 4(b) provide a schematic description of the controller implementation for single-phase and three-phase inverters, respectively.

As outlined in [11], [12], a straightforward design procedure for the oscillator parameters has been developed. With reference to Fig. 4, oscillations at the desired frequency, ω_{rated}, are obtained by selecting R, L, and C such that $\omega_{\text{rated}} = \sqrt{1/(LC)}$ and $\sigma > 1/R$. The voltage scaling gain, ν, is chosen as $\nu = \sqrt{2}V_{\text{rated}}$, where V_{rated} denotes the RMS rated voltage of the ac power system. The controller parameters φ and ι are tuned such that the voltage across the inverter output terminals stays within predefined upper and lower voltage limits across the entire load range. Once the values of R, L, C, σ, φ, ι, and ν are computed, they are utilized by all virtual oscillators in the system.

Unique power ratings for the inverters are accommodated by selecting the values of κ in proportion to the inverter power ratings. Given the j^{th} and k^{th} inverters with power ratings P_j and P_k, respectively, it can be shown that if κ_j and κ_k are selected such that

$$\frac{P_j}{\kappa_j} = \frac{P_k}{\kappa_k}, \tag{1}$$

then the inverters share the load power in proportion to their ratings [12]. In deriving the result in (1), it was assumed that the per-unitized filter impedance of each inverter is identical such that the filter impedance of the j^{th} inverter

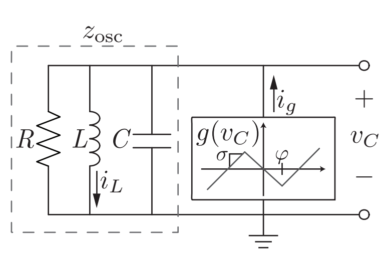

Fig. 1. Schematic of a single dead-zone oscillator.

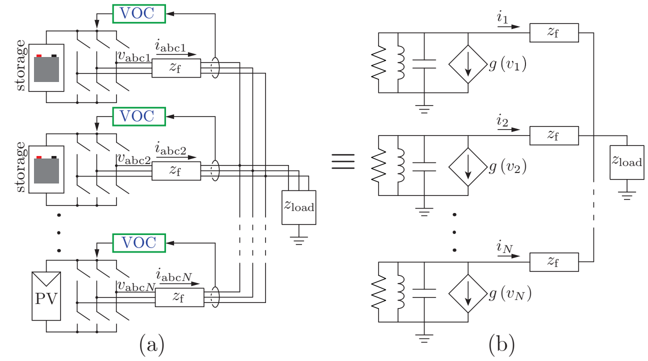

Fig. 2. Microgrid composed of parallel three-phase inverters in (a) is controlled to emulate the corresponding single-phase system of coupled oscillators in (b). The current and voltage gains that interface the virtual oscillators to the parallel inverters are not depicted for conciseness.

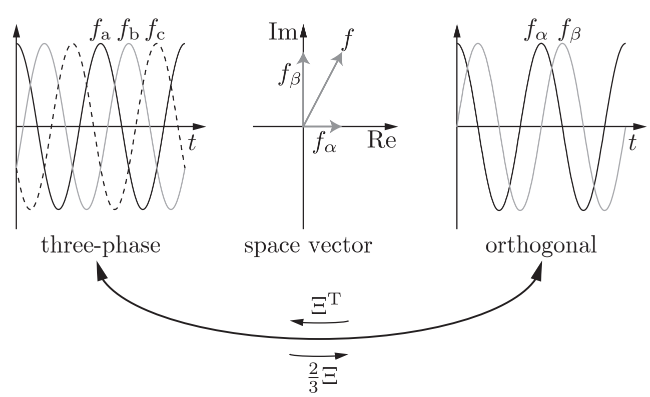

Fig. 3. Illustration of the α-β transformation and its inverse. For a set of balanced three-phase signals, f_{a}, f_{b}, and f_{c}, the corresponding *space vector* signal is given by $f := \frac{2}{3}\left(f_{\text{a}} + f_{\text{b}}\mathrm{e}^{\frac{-2\pi}{3}\mathrm{j}} + f_{\text{c}}\mathrm{e}^{\frac{2\pi}{3}\mathrm{j}}\right)$. The real and imaginary components of f are denoted by f_α and f_β, respectively. Coordinate transformations between the three-phase and orthogonal signals are effected by using the matrix, Ξ.

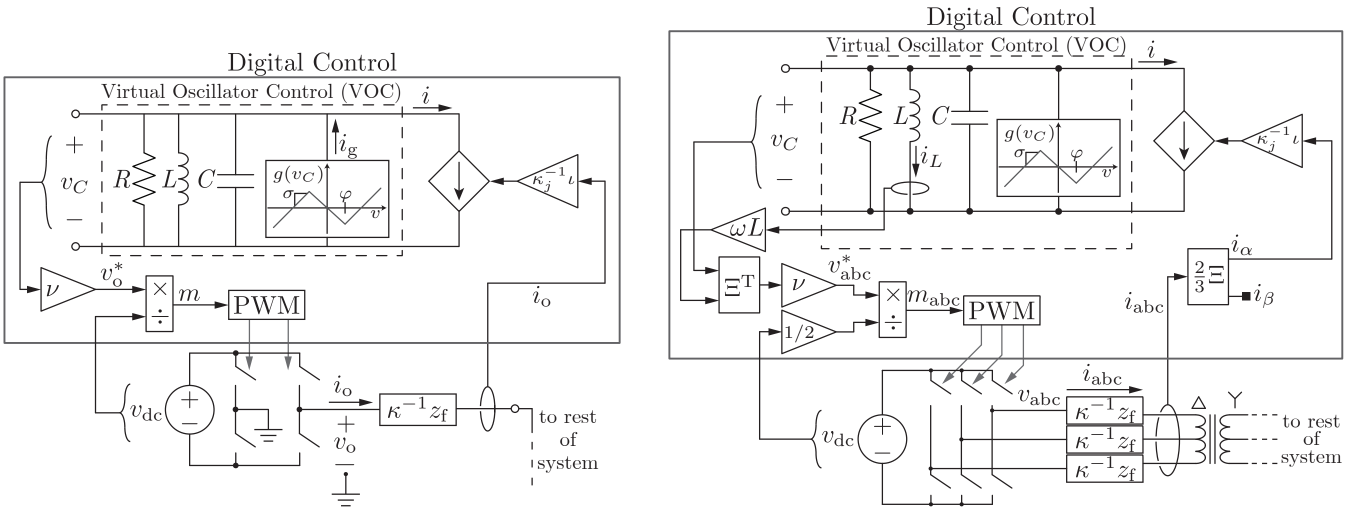

(a) (b)

Fig. 4. Implementation of the proposed controller for (a) single-phase and (b) three-phase voltage-source inverters.

can be expressed as $\kappa_j^{-1} z_f$, as illustrated in Fig. 4. In practice, this filter design strategy also ensures that the relative distortion generated by each inverter also scales with its power rating [29].

The three-phase controller employs an α-β coordinate transformation, captured by the matrix

$$\Xi := \begin{bmatrix} 1 & -\frac{1}{2} & -\frac{1}{2} \\ 0 & \frac{\sqrt{3}}{2} & -\frac{\sqrt{3}}{2} \end{bmatrix}. \tag{2}$$

Figure 3 illustrates the coordinate transformation described above for a representative set of three-phase signals. The orthogonality of the virtual-oscillator capacitor voltage and inductor currents is leveraged to generate the three-phase PWM switching waveforms. Further details pertaining to controller implementation for the single- and three-phase inverters are in [12] and [11], respectively. Finally, it is worth mentioning that for analytical purposes, the physical system in Fig. 2(a) can be modeled by the equivalent model of coupled nonlinear dead-zone oscillators in Fig. 2(b).

III. Global Asymptotic Synchronization

In a parallel system of identical inverters connected to a common load, the terminal voltages of the inverters must synchronize. Given the correspondence between the physical system of inverters and the virtual nonlinear oscillators depicted in Fig. 2, this translates equivalently to requiring the terminal voltages of the virtual oscillators to synchronize. In [10], we derived the following condition for global asymptotic synchronization for the virtual-oscillator terminal voltages:

$$\max_{\omega} \left\| \frac{z_f(j\omega) z_{osc}(j\omega)}{z_f(j\omega) + z_{osc}(j\omega)} \right\|_2 \sigma < 1, \tag{3}$$

where z_{osc} is the oscillator impedance (corresponding to the parallel *RLC* circuit, i.e., $z_{osc} = R \| j\omega L \| (j\omega C)^{-1}$), z_f is the series output-filter impedance, and σ is the maximum slope of the function $g(\cdot)$ that governs the nonlinear voltage-dependent current source. This result was first applied to linear (passive impedance) loads, and with unity current and voltage gains (i.e., $\iota = 1$ and $\nu = 1$). In [12], the result was extended to accommodate nonlinear loads and arbitrary current and voltage gains to obtain the following synchronization condition:

$$\max_{\omega} \left\| \frac{(\nu\iota)^{-1} z_f(j\omega) z_{osc}(j\omega)}{(\nu\iota)^{-1} z_f(j\omega) + z_{osc}(j\omega)} \right\|_2 \sigma < 1, \tag{4}$$

It is interesting to note that despite allowing for distinct power ratings among inverters, the synchronization condition in (4) does not depend on the value of κ for any inverter.

The synchronization conditions in (3)-(4) present several appealing features. First, notice that the synchronization conditions are independent of the load, the number of (virtual) oscillators, and their power ratings. From an application perspective, this implies that with VOC, synchronization in the power system can be ensured without any knowledge about the load parameters and the number of participating inverters. The most attractive feature of the proposed VOC paradigm is that these favorable system-level properties—power sharing, synchronization conditions being independent of load and number of inverters—are guaranteed with no communication.

IV. Case Studies

In this section, we provide a simulation case study to demonstrate the application of VOC in a system of three parallel connected three-phase inverters serving a constant-power load. The inverters in the system have ratings of 7.5 kW, 15 kW, and 30 kW such that the parallel inverters share the load current according to a ratio of 1 : 2 : 4. The specifications of the inverters and controllers are provided in the Appendix and it can be verified that the synchronization condition in (4) is satisfied. As illustrated in Fig. 6, the load is

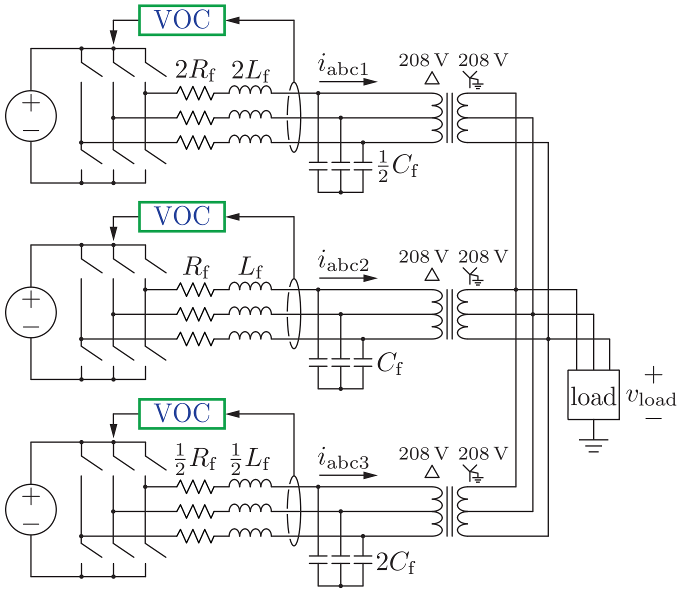

Fig. 5. Schematic of parallel inverter system used in simulation case study. The three inverters are connected in parallel across a constant power load.

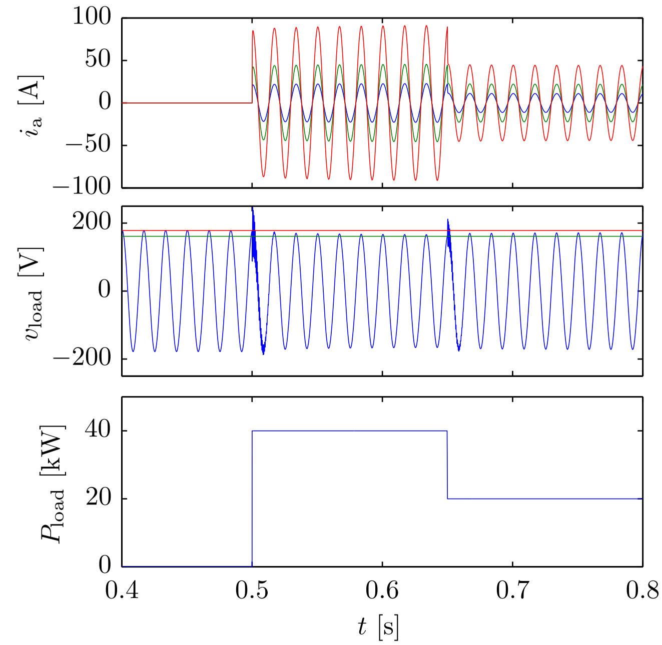

Fig. 6. Simulation results for a system consisting of three parallel three-phase inverters connected across a constant power load. Inverters #1, #2, and #3, have power ratings of 7.5 kW, 15 kW, and 30 kW, respectively. The oscillator-based controllers are designed such that each inverter shares the load in proportion to its rating. Waveforms corresponding to inverter phase *a* output currents, load voltage, and load power are depicted.

initially consuming no power and then undergoes a series of step changes. Despite the relatively large load transients, the load voltage stays within ±5% of the nominal value (bounds are depicted in Fig. 6).

V. Conclusions

This paper summarized a suite of methods that have recently been proposed for the control and synchronization of parallel single- and three-phase voltage source power electronics inverters. Inspired by the phenomenon of synchronization in networks of coupled oscillators, the premise of the virtual oscillator control is to modulate inverter operation to mimic the dynamics of nonlinear oscillators. Simulation results were provided to demonstrate applications of the proposed control method in a system of three-phase inverters serving a constant power load.

Appendix

Electrical network and inverter-design parameters

Oscillator linear-subsystem parameters: $R = 10\,\Omega$, $L = 250\,\mu$H, $C = 28.14$ mF. Oscillator nonlinear-subsystem parameters: $\sigma = 1$ S, $\varphi = 0.47$ V. Inverter voltage gain and current gain: $\nu = 208\sqrt{1/3}$ and $\iota = 1.0568 \times 10^{-3}$, respectively. Nominal inverter output filter parameters: $R_f = 0.1\,\Omega$, $L_f = 250\,\mu$H, $C_f = 24\,\mu$F. Inverter power ratings and corresponding scaling paramaters: $P_1 = 7.5$ kW, $\kappa_1 = 1/2$, $P_2 = 15$ kW, $\kappa_2 = 1$, $P_3 = 30$ kW, $\kappa_3 = 2$.

Acknowledgment

The authors would like to acknowledge Professor P. T. Krein, who is a co-author on [10]–[12].

References

[1] J.-F. Chen and C.-L. Chu, "Combination voltage-controlled and current-controlled PWM inverters for UPS parallel operation," *IEEE Trans. Power Electron.*, vol. 10, pp. 547–558, Sept. 1995.

[2] Y. Xue, L. Chang, S. B. Kjaer, J. Bordonau, and T. Shimizu, "Topologies of single-phase inverters for small distributed power generators: An overview," *IEEE Trans. Power Electron.*, vol. 19, pp. 1305–1314, Sept. 2004.

[3] Y. A. R. I. Mohamed and E. El-Saadany, "Adaptive decentralized droop controller to preserve power sharing stability of paralleled inverters in distributed generation microgrids," *IEEE Trans. Power Electron.*, vol. 23, pp. 2806–2816, Nov. 2008.

[4] D. De and V. Ramanarayanan, "Decentralized parallel operation of inverters sharing unbalanced and nonlinear loads," *IEEE Trans. Power Electron.*, vol. 25, pp. 3015–3025, Dec. 2010.

[5] B. Johnson, A. Davoudi, P. Chapman, and P. Sauer, "Microgrid dynamics characterization using the automated state model generation algorithm," in *IEEE Proc. Int. Symp. on Circuits and Syst.*, pp. 2758–2761, June 2010.

[6] B. Johnson, A. Davoudi, P. Chapman, and P. Sauer, "A unified dynamic characterization framework for microgrid systems," *Electric Power Components and Systems*, vol. 40, pp. 93–111, Nov. 2011.

[7] R. Bojoi, L. Limongi, D. Roiu, and A. Tenconi, "Enhanced power quality control strategy for single-phase inverters in distributed generation systems," *IEEE Trans. Power Electron.*, vol. 26, pp. 798–806, Mar. 2011.

[8] M. Borrega, L. Marroyo, R. Gonzalez, J. Balda, and J. Agorreta, "Modeling and control of a master-slave PV inverter with N-paralleled inverters and three-phase three-limb inductors," *IEEE Trans. Power Electron.*, vol. 28, pp. 2842–2855, June 2013.

[9] L. A. B. Tôrres, J. P. Hespanha, and J. Moehlis, "Power supplies synchronization without communication," in *Proc. of the Power and Energy Society General Meeting*, July 2012.

[10] B. B. Johnson, S. V. Dhople, A. O. Hamadeh, and P. T. Krein, "Synchronization of nonlinear oscillators in an LTI electrical network," *IEEE Trans. Circuits Syst. I: Fundam. Theory Appl.*, 2013. To Appear.

[11] B. B. Johnson, S. V. Dhople, J. L. Cale, A. O. Hamadeh, and P. T. Krein, "Oscillator-based inverter control for islanded three-phase microgrids," *IEEE Journ. Photovoltaics*, 2013. To appear.
[12] B. Johnson, S. Dhople, A. Hamadeh, and P. Krein, "Synchronization of parallel single-phase inverters using virtual oscillator control," *IEEE Trans. Power Electron.*, 2013. In review.
[13] M. Chandorkar, D. Divan, and R. Adapa, "Control of parallel connected inverters in standalone ac supply systems," *IEEE Trans. Ind. Appl.*, vol. 29, pp. 136–143, Jan. 1993.
[14] R. Lasseter, "Microgrids," in *IEEE Power Eng. Society Winter Meeting*, vol. 1, pp. 305–308, 2002.
[15] M. Marwali, J.-W. Jung, and A. Keyhani, "Control of distributed generation systems - Part II: Load sharing control," *IEEE Trans. Power Electron.*, vol. 19, pp. 1551–1561, Nov. 2004.
[16] P. Piagi and R. Lasseter, "Autonomous control of microgrids," in *IEEE Power Eng. Society General Meeting*, vol. 6, pp. 1–8, June 2006.
[17] K. De Brabandere, B. Bolsens, J. Van den Keybus, A. Woyte, J. Driesen, and R. Belmans, "A voltage and frequency droop control method for parallel inverters," *IEEE Trans. Power Electron.*, vol. 22, pp. 1107–1115, July 2007.
[18] J. Kim, J. Guerrero, P. Rodriguez, R. Teodorescu, and K. Nam, "Mode adaptive droop control with virtual output impedances for an inverter-based flexible ac microgrid," *IEEE Trans. Power Electron.*, vol. 26, pp. 689–701, Mar. 2011.
[19] J. Rocabert, A. Luna, F. Blaabjerg, and P. Rodriguez, "Control of power converters in ac microgrids," *IEEE Trans. Power Electron.*, vol. 27, pp. 4734–4749, Nov. 2012.
[20] C.-T. Lee, C.-C. Chu, and P.-T. Cheng, "A new droop control method for the autonomous operation of distributed energy resource interface converters," *IEEE Trans. Power Electron.*, vol. 28, pp. 1980–1993, Apr. 2013.
[21] J. Guerrero, L. de Vicuna, J. Matas, M. Castilla, and J. Miret, "A wireless controller to enhance dynamic performance of parallel inverters in distributed generation systems," *IEEE Trans. Power Electron.*, vol. 19, pp. 1205–1213, Sept. 2004.
[22] J. Lopes, C. Moreira, and A. Madureira, "Defining control strategies for microgrids islanded operation," *IEEE Trans. Power Syst.*, vol. 21, pp. 916–924, May 2006.
[23] N. Pogaku, M. Prodanovic, and T. C. Green, "Modeling, analysis and testing of autonomous operation of an inverter-based microgrid," *IEEE Trans. Power Electron.*, vol. 22, pp. 613–625, Mar. 2007.
[24] J. M. Guerrero, J. C. Vasquez, J. Matas, L. G. de Vicuña, and M. Castilla, "Hierarchical control of droop-controlled AC and DC microgrids–a general approach toward standardization," *IEEE Trans. Ind. Electron.*, vol. 58, no. 1, pp. 158–172, 2011.
[25] J. He and Y. W. Li, "An enhanced microgrid load demand sharing strategy," *IEEE Trans. Power Electron.*, vol. 27, pp. 3984–3995, Sept. 2012.
[26] Q.-C. Zhong, "Robust droop controller for accurate proportional load sharing among inverters operated in parallel," *IEEE Trans. Ind. Electron.*, vol. 60, pp. 1281–1290, April 2013.
[27] H. Khalil, *Nonlinear Systems*. Upper Saddle River, NJ: Prentice Hall, third ed., 2002.
[28] A. Mauroy, P. Sacré, and R. J. Sepulchre, "Kick synchronization versus diffusive synchronization," in *IEEE Conference on Decision and Control*, pp. 7171–7183, 2012.
[29] B. Parikshith and V. John, "Higher order output filter design for grid connected power converters," in *National Power Systems Conf.*, vol. 1, pp. 614–619, Dec. 2008.